MECOM permits pancreatic acinar cell dedifferentiation avoiding cell death under stress conditions

Running title: MECOM permits acinar cell dedifferentiation

Backx Elyne [1], Wauters Elke [2], Baldan Jonathan[2], Van Bulck Mathias[1], Michiels Ellis[1], Heremans Yves[1,3], De Paep Dieter Luc [4], Bouwens Luc [2], Kurokawa Mineo [5], Goyama Susumu [5], Jacquemin Patrick [6], Houbracken Isabelle[1,2], Rooman Ilse[1]

[1] Laboratory of Medical and Molecular Oncology, Oncology Research Centre, Vrije Universiteit Brussel, Brussels, Belgium

[2] Cell Differentiation Laboratory, Vrije Universiteit Brussel, Brussels, Belgium

[3] Laboratory of Beta Cell Neogenesis, Vrije Universiteit Brussel, Brussels, Belgium

[4] Beta Cell Bank, Diabetes Research Center, UZ Brussel, Brussels, Belgium

[5] Department of Hematology and Oncology, Graduate School of Medicine, The University of Tokyo, Tokyo, Japan

[6] Laboratory of Liver and Pancreatic Differentiation, De Duve Institute, Université Catholique de Louvain, Brussels, Belgium

Corresponding author: Ilse Rooman, irooman@vub.be

ABSTRACT

Maintenance of the pancreatic acinar cell phenotype suppresses tumor formation. Hence, repetitive acute or chronic pancreatitis, stress conditions in which the acinar cells dedifferentiate, predispose for cancer formation in the pancreas. Dedifferentiated acinar cells acquire a large panel of duct cell specific markers. However, it remains unclear to what extent dedifferentiated acini differ from native duct cells and which genes are uniquely regulating acinar cell dedifferentiation. Moreover, most studies have been performed in mouse since the availability of human cells is scarce.

Here, we applied a non-genetic lineage tracing method in our culture model of human pancreatic exocrine cells that allowed cell-type specific gene expression profiling by RNA sequencing. Subsequent to this discovery analysis, one transcription factor that was unique for dedifferentiated acinar cells was functionally characterized using *in vitro* and *in vivo* genetic loss-of-function experimental models.

RNA sequencing analysis showed that human dedifferentiated acinar cells expressed genes in 'Pathways of cancer' with prominence of the transcription factor *MECOM (EVI-1)* that was absent from duct cells. During mouse embryonic development, pre-acinar cells transiently expressed MECOM and MECOM was re-expressed in experimental *in vivo* models of acute and chronic pancreatitis *in vivo,* conditions in which acinar cells dedifferentiate. MECOM expression correlated with and was directly regulated by SOX9. MECOM loss-of-function in mouse acinar cells *in vitro* and *in vivo* impaired cell adhesion resulting in more prominent acinar cell death and suppressed acinar cell dedifferentiation by limiting ERK signaling.

In conclusion, we transcriptionally profiled the two major human pancreatic exocrine cell types, acinar and duct cells, during experimental stress conditions. We provide insights that in dedifferentiated acinar cells, cancer pathways are upregulated in which

MECOM is a critical regulator that suppresses acinar cell death by permitting cellular dedifferentiation.

INTRODUCTION

Few cancers have such poor survival rates as pancreatic ductal adenocarcinoma (PDAC) (1). Understanding the molecular mechanisms that are at play in early stage cancer formation is important to improve disease outcomes, but clinical samples of early disease are rare. Hence, genetically modified mouse models are pivotal to provide us insight into the contribution of the different pancreatic cell types to tumor formation (2-4). Accumulating evidence points to acinar cells as cells of origin for pancreatic tumor development (5-10). In order to become susceptible to tumorigenesis, acinar cells have to lose their differentiated phenotype to some extent. Consequently, tumorigenesis. is restrained by mechanisms that control acinar cell differentiation (5-10). Loss of differentiation can result from repetitive acute or chronic pancreatitis whereby dedifferentiated acinar cells acquire a panel of markers that are typical for (embryonic) duct cells (11-13). Notably, duct cells can also give rise to tumors but likely through on other mechanisms (14-16).

To date, knowledge is lacking to discriminate the mechanisms that govern the duct-like dedifferentiated acinar cell phenotype versus the ‘native’ duct cell phenotype, the latter being more resistant to stress- or inflammation-associated tumorigenesis. Previously, we had established *in vitro* experimental models that recapitulate a human (12) and rodent (13) acinar dedifferentiation. Specifically, upon suspension culture acinar cells lose their acinar-specific markers while gaining (embryonic) duct-like features, thereby mimicking chronic pancreatitis(12, 13).Here, we investigated the differential gene expression in adult human dedifferentiated acinar cells compared to

71 native duct cells from the same cell preparations. The transcription factor *MECOM/EVI-*
72 *1* was found to be uniquely re-expressed in dedifferentiated acinar cells since
73 embryonic development.
74 Although *MECOM* transcription factor is a known oncogene with a role in apoptosis
75 (17-19) and pancreatic tumor formation (20, 21), its function in acinar cell
76 (de)differentiation is still unknown. We analyzed its role in the context of acinar cell
77 dedifferentiation through caerulein-induced pancreatitis modeling in transgenic *Evi-1*
78 knock-out mice. We provide mechanistic insights that mouse acinar cells are
79 dependent on MECOM expression to prevent cell death by allowing them acquisition
80 of the dedifferentiated cell state.
81

82 **MATERIALS AND METHODS**

83 **Human donor material and cell culture**

84 Human pancreata from deceased donors were processed by the Beta Cell Bank of
85 the Centre for Beta Cell Therapy in Diabetes (Brussels, Belgium), affiliated to the
86 Eurotransplant Foundation (Leiden, The Netherlands). Consent for the use of
87 residual donor material for research was obtained according to the legislation in
88 country of organ procurement. This project was approved by the Medical Ethical
89 Committee of UZ Brussel - Vrije Universiteit Brussel (B.U.N. 143201732260).
90 Human exocrine cells were cultured as previously described (11, 12).
91

92 **Mouse strains and experiments**

93 ElaCreERT mice (22) ElaCreERT;Sox9$^{f/f}$ (23) (kindly provided by P. Jacquemin (UCL,
94 Belgium) originally from D. Stoffers (UPenn, USA)) were crossed with EVI-1exon4 loxP
95 mice (*Mecom*$^{f/f}$) (24) (kindly provided by M. Kurokawa, UPenn), resulting in

96 ElaCreERT;*Mecom*$^{f/f}$ mice (Mecom KO). ElaCreERT;*Sox9*$^{f/f}$ (23) were kindly provided
97 by P. Jacquemin (UCL, Belgium). Six to eight-weeks-old ElaCreERT;*Mecom*$^{f/f}$ and
98 ElaCreERT;Sox9$^{f/f}$ mice received tamoxifen and (Z)-4-Hydroxytamoxifen (all from
99 Sigma-Aldrich, St-Louis, MO, USA) and were treated with 1,25mg/kg body weight
100 caerulein (Invitrogen Waltham, Massachusetts, USA) according to (23). Acinar cell
101 isolation was adapted from (13). Embryonic mouse tissue was isolated from
102 ElaCreERT mice at E16.5 timepoint of embryonic development. All animal experiments
103 were approved by the Ethical Committee for Animal Testing at the Vrije Universiteit
104 Brussel (#17-637-1).
105
106 **Fluorescent activated cell sorting (FACS)**
107 FITC-conjugated UEA-1 (*Ulex Europaeus* Agglutinin-1, Sigma-Aldrich) lectin labeling
108 of acinar cells within the human exocrine cell fraction was performed as in (12). At day
109 4 of suspension culture, cell clusters were dissociated following the protocol of (11).
110 Analysis and cell sorting were performed on a BD FACSAria (BD Biosciences, Franklin
111 Lakes, NJ, USA). Viable, single cells were gated based on forward and side scatter.
112
113 More details on experimental design and statistics can be found in supplementary
114 materials and methods.
115
116 **Results**
117 **MECOM is a cancer-related transcription factor uniquely expressed in human**
118 **dedifferentiated acinar cells**
119 Given the difference in propensity of dedifferentiated acinar cells and duct cells for
120 pancreatitis-associated tumor development (5), we were specifically interested in the

121 differential gene expression of these two populations. Using the acinar-specific UEA-
122 1 lectin in combination with the duct cell marker CA19.9, we FACS-purified both cell
123 populations (11, 12) (Figure 1a,b). We confirmed the mutually exclusive expression
124 pattern of CD142, a progenitor marker (11) in the UEA1+ dedifferentiated acinar cells,
125 and of CA19.9 in the UEA1- duct cells (Figure 1b). We validated the different
126 expression levels of the acinar cell markers MIST-1 and chymotrypsin, the progenitor
127 marker CD142 and the duct-cell marker CK19 in the original mixed exocrine cell
128 fraction and in the purified dedifferentiated acinar cells (UEA1+/CA19.9-) and native
129 duct cells (UEA1-/CA19.9+) (Supplementary Figure 1). Comparing dedifferentiated
130 acinar cells with native duct cells by RNAseq analysis highlighted 7953 differentially
131 expressed genes (Adj. p<0,01). Of these, 1219 genes were expressed higher in
132 dedifferentiated acinar cells (log fold change (FC) of ≤-2; Adj. p<0,01) (Supplementary
133 Table 1) and were enriched for the KEGG pathways (Adj. p<0.01): 'Protein digestion
134 and absorption' and 'Pancreatic secretion', including genes such as carboxypeptidase
135 A and amylase, pointing to gene expression reminiscent of the abundant acinar cell
136 transcriptome (25). In addition, 'Pathways in cancer' belonged to the top enriched
137 pathways such as those of the WNT signaling pathway, which is well-known for its
138 function in pancreatic tumorigenesis. Other enriched pathways included 'PI3K-AKT
139 signaling', which is involved in acinar cell dedifferentiation and pancreatic
140 tumorigenesis (26-28) and 'Complement and coagulation cascades' encompassing
141 genes belonging to the tissue damage pathway (Figure 1c) and that code for F8,
142 fibrinogen and F3 (CD142), the marker used above (11) (Figure 1b).
143 Dedifferentiated acinar and duct cells did have equal expression of the embryonic
144 precursor gene *PDX1*, confirming our previous work (13). *PTF1A*, *NR5A2*, *RBPJL*,
145 *FOXA3* and *GATA4* were expressed higher in the dedifferentiated acini reminiscent of

146 their fully differentiated state. Of note, *GATA6* expression, which is required for
147 embryonic acinar cell differentiation (29, 30) and a suppressor of pancreatic
148 carcinogenesis (31, 32), was not different from the duct cells.
149 Conversely, duct cell-enriched genes included *CFTR*, *SOX9*, *NKX6.1*, *HES1*, *HNF1B*
150 and *ONECUT2* (*HNF6B*), established markers of duct cell differentiation. The most
151 significantly duct cell-enriched gene was *DCDC2* (Doublecortin Domain Containing 2),
152 demonstrated to bind tubulin and enhance microtubule polymerization (33) (Figure 1d).
153 In the duct cell fraction, we found KEGG pathway enrichment for 'ECM receptor
154 pathway interaction' and 'O-linked glycosylation'. Also, here, 'Pathways in cancer'
155 featured here but the genes in this pathway differed from the ones in the
156 dedifferentiated acinar cell fraction (Supplementary Table 1).
157 Among the differentially expressed genes were 71 transcription factors. The most
158 significantly enriched transcription factor in the dedifferentiated acinar cell fraction was
159 *MECOM* (log2FC = -6,09; Adj. p = 1,04E-123) (Figure 1d, Supplementary Table 1).
160 *MECOM*, a known oncogene (34-36). It has been described as an activator of KRAS
161 and glypican-1 in pancreatic cancer (20, 21). During our study, it was reported in
162 relation to acinar cell-derived tumorigenesis (37). Hence, we confirmed *MECOM*
163 expression in human PDAC samples (N=3) (Supplementary Figure 2a). We also used
164 RNAseq analysis of stage 1 and 2 PDAC (N=103) where it correlated positively with
165 overall survival (Supplementary figure 2b). In the same cohort, we previously reported
166 a similar pattern for *SOX9* and a correlation in expression between *SOX9* and *MECOM*
167 (Pearson R=0,49) (23). Pathway analysis of genes correlating with MECOM
168 (Supplementary figure 2c) revealed similar pathways as those reported in our study on
169 SOX9 where regulation of ErbB signaling was highlighted (23).

170 In conclusion, we FACS-purified human dedifferentiated acinar and duct cells and
171 analyzed their transcriptome. The dedifferentiated acinar cell fraction showed a
172 signature reminiscent of the acinar cell identity and specifically expressed *MECOM*, a
173 transcription factor that featured in the pathway 'Pathways of cancer'. MECOM was
174 expressed in PDAC where it correlated with SOX9. We hypothesized that MECOM
175 plays a role during acinar cell dedifferentiation, an event that initiates pancreatic tumor
176 development.
177
178 **MECOM is expressed in developing acinar cells and is re-expressed during**
179 **pancreatitis-associated acinar cell dedifferentiation**
180 We comprehensively assessed expression of MECOM during acinar cell differentiation
181 or loss thereof.
182 First, we confirmed the differential expression of *MECOM* in the purified human
183 dedifferentiated acinar and duct cells from the experiments above (Figure 2a). Using
184 RISH, *MECOM* mRNA appeared expressed at low levels in the acinar compartment of
185 normal human pancreas (0,24±0,09 mRNA dots/cell; N=3), but increased strongly in
186 samples of chronic pancreatitis (1,46±0,10 mRNA dots/cell; N=3) (Figure 2b,c).
187 Within the human purified dedifferentiated acinar cell fraction, *MECOM* showed strong
188 correlation with *CD142* (Pearson R = 0,926, adj. P < 0,01), as discussed before (Figure
189 1). Immunofluorescent co-staining of MECOM and CD142 after 4 days of culture
190 showed strong colocalization of the two proteins (56,94±10,63% MECOM+/CD142+
191 cells; N=5), while MECOM did not co-localize with the duct cell marker CK19
192 (5,69±2,32% MECOM+/CK19+ cells; N=5) (Figure 2d,e).
193 Next, we assessed the expression pattern (Figure 2f-i) and levels (Figure 2j) of *Mecom*
194 mRNA in murine pancreas. In contrast to normal adult mouse pancreas where *Mecom*

195 was expressed at very low levels (Figure 2f,j) a significantly increased expressed was
196 noted in E16.5 pancreas where it localized to pro-acinar tip cells (Figure 2g,j) (38, 39).
197 Similar to human, *Mecom* became re-expressed during acute and chronic pancreatitis
198 in mouse (Figure 2h,i,j).
199 Altogether, these data show that *Mecom* is transiently expressed in developing acinar
200 cells and becomes re-expressed during pancreatitis in dedifferentiated acinar cells.
201
202 **SOX9 regulates *Mecom* expression in dedifferentiated acinar cells**
203 SOX9 is an important marker of acinar cell dedifferentiation and is indispensable for
204 tumor formation in the pancreas (23). SOX9 correlates with MECOM in PDAC patients,
205 as shown above, but also in other tissues (40, 41). Hence, we investigated whether
206 these two transcription factors might also correlate in the context of acinar cell
207 dedifferentiation. Indeed, we observed a strong correlation between *MECOM* and
208 *SOX9* (Pearson R = 0,83; *p=0,015; N=6) (Figure 3a) in the human exocrine cell
209 cultures in which acinar cells gradually dedifferentiate, a finding which was confirmed
210 at the protein level (Figure 3b).
211 Based on the observed induction of *Mecom* after 48 hours of caerulein-induced acute
212 pancreatitis (Figure 2h), we investigated *Mecom* expression in *Sox9* loss-of-function
213 mice (Figure 3c) (13, 42). ElaCreERT;*Sox9*$^{f/f}$ mice showed significant reduction in
214 *Mecom* compared to control mice (ElaCreERT) (19,48 ± 4,54% reduction in mRNA
215 dots) (Figure 3c). suggestive for SOX9 to act as an upstream regulator of *Mecom*.
216 To further study whether SOX9 directly regulated *Mecom* in the acinar cell context, we
217 performed a promoter-reporter assay on the partially differentiated mouse acinar cell
218 line 266-6 (that expresses *Mecom*, as shown further). We observed low increase in
219 luciferase activity when cells were transfected with the *Mecom* enhancer expression

220 plasmid alone. After *Sox9* overexpression, luciferase activity increased significantly
221 (Figure 3d), indicating that SOX9 regulates the Mecom enhancer in partially
222 differentiated acinar cells.
223 In conclusion, we showed that *Mecom* is (directly) regulated by SOX9 in pancreatic
224 acinar cell context.
225
226 ***Mecom* maintains cell adhesion and cell viability in a partially differentiated**
227 **acinar cell line and in human and mouse acinar cell cultures**
228 A lentiviral all-in-one CRISPR/Cas9-mediated approach comparing 3 different gRNAs
229 designed to knock out (KO) *Mecom* in a partially differentiated acinar cell line (266-6)
230 (Supplementary Figure 3), enabled us to study the role of Mecom in acinar cell
231 dedifferentiation. RISH for *Mecom* in the loss-of-function condition (Figure 4a) showed
232 significant reduction of mRNA expression (27,30±4,25% dots/cell decrease). In the
233 Mecom KO condition, the cells were not able to organize into the typical 'acinar dome-
234 like' structures that were observed in the cells transduced with non-targeting gRNA
235 (Figure 4b), suggestive of loss of proper cell-cell contacts. We also observed a
236 decrease in absolute cell number (Figure 4c), an overall diminished cell viability (Figure
237 4d) and a significant increase in cleaved caspase 3+ cells (Figure 4e), all indicative of
238 cell death.
239 We further studied downstream transcriptional effects of Mecom loss in this cell line by
240 RNAseq analysis. Differential gene expression analysis revealed downregulation of
241 genes enriched in 'Focal adhesion', 'ECM receptor interaction' and 'Pathways in
242 cancer' (Figure 4f). This supported our observations of diminished dome formation due
243 to potentially impaired cell adhesion. We also compared the differentially expressed
244 genes from the Mecom KO condition with a publicly available MECOM ChIP-Seq

245 dataset (43) and found several overlapping genes (Figure 4g) that we further
246 considered, in particular integrins that link the extracellular matrix (ECM) components
247 such as collagen to the cytoskeleton. The data suggested that loss of *Mecom* might
248 compromise cell-cell interaction by diminished Collagen IV-Integrin a2 interaction and
249 downstream ERK-mediated signaling (Figure 4h), the latter considered crucial in acinar
250 cell dedifferentiation (44).
251 Diminished expression of collagen type IV and reduced ERK signaling upon Mecom
252 loss-of-function was confirmed by immunofluorescent staining (Figure 4i,j).
253 In conclusion, *Mecom* is indispensable to maintain cell adhesion and cell viability in a
254 partially differentiated acinar cell line.
255 Next, we crossed ElaCreERT deletor mice with mice carrying a floxed exon 4 of *Evi*,
256 an exon which is conserved in all transcript variants (24) (Figure 5a). We studied
257 effects in dedifferentiated acinar cells isolated from these mice using an established
258 cell culture model, similar to the human cell culture model described above (13).
259 Immunohistochemical staining for MECOM showed 42,71±13,42% less MECOM
260 positive cells in freshly isolated (day 0) MECOM KO exocrine cells, consistent with
261 previous reports on the recombination efficiency of the ElaCreERT strain (45-47).
262 Interestingly, by day 4, we detected only 23,89±13,42% less MECOM positive cells in
263 the KO condition suggesting selective loss of MECOM deficient cells (Supplementary
264 Figure 4).
265 We observed that after cell isolation the control cells remained organized in small
266 acinar spheroid-like structures while in the MECOM KO condition they often presented
267 as single cells. After 4 days of culture, clusters did form in the ElaCreERT;*Mecom*$^{f/f}$
268 mouse cells but cluster diameter was significantly smaller compared to those of
269 ElaCreERT control mice (57,21±15,73% reduction in average diameter) (Figure 5b,e),

270 suggestive of diminished cell adhesion and cell death of the single cells. In our
271 experience acinar cells cannot survive as single cells (e.g. after FACS purification).
272 Similar to our results in the 266-6 cells (Figure 4), an increased fraction of acinar cells
273 in the MECOM KO cultures stained positive for cleaved caspase 3 (81,21±26,47%
274 increase in cleaved caspase 3+ cells) (Figure 5c,f). Notably, the MECOM KO cultures
275 also showed fewer expression of CK19+ cells in comparison to the control cells
276 (25,79±6,33% reduction in CK19+ cells), suggesting a lower capacity for
277 dedifferentiation (Figure 5d,g).
278 These observations were confirmed by shRNA-mediated knockdown in cultured
279 human exocrine cells in culture. At 24h, 4 and 7 days after transduction, average
280 cluster diameter was significantly decreased (Supplementary Figure 5), underscoring
281 the compromised cell-cell adhesion.
282 In conclusion, MECOM is indispensable for maintenance of cell-cell adhesion and cell
283 viability in primary cultures of mouse and human acinar cells.
284

285 **Mice with *Mecom*-deficient acinar cells show impaired recovery from acute**
286 **pancreatitis**

287 Since the primary cell culture models above recapitulate acinar cell dedifferentiation
288 as it occurs during pancreatitis (11-13), we subjected control and MECOM KO mice to
289 caerulein-induced acute pancreatitis. In wild-type mice, acute pancreatitis peaks
290 around day 4 and resolves by day 11 (Figure 6a). We observed no macroscopic
291 differences in the pancreas nor in weight of the pancreas or body weight when
292 comparing Mecom-deficient with control mice (Supplementary Figure 6).
293 Haematoxylin-eosin staining however showed more inter-acinar spaces at day 11 in
294 the Mecom KO mice (Figure 6b,f). Similar to the phenotype observed in the 266-6 cells

295 (Figure 4) and the *ex vivo* cultures (Figure 5), this was preceded by an increased
296 incidence of apoptosis (Figure 6c,g). Since we observed more inter-acinar space in the
297 Mecom KO mice, we analyzed immune cell infiltration. Similar to a previous report (37),
298 at day 11, CD3 positive area in MECOM KO mice remained at a level comparable to
299 the acute phase of pancreatitis (day 4) whereas in the control mice it was significantly
300 decreased (Figure 6e,i). F4/80+ macrophages showed a similar trend (not shown).
301 Remarkably, no difference in collagen deposition could be detected between control
302 and MECOM KO mice (Figure 6d,h) indicating that the inter-acinar space was not filled
303 with collagen. The histological pattern showing accumulation of excessive liquid in the
304 interstitial space was consistent with that of edema. Also, we did not observe any
305 changes in acinar-to-ductal transdifferentiation markers at day 11 (not shown).
306 Altogether, these results indicate that MECOM-deficiency in pancreatic acinar cells
307 under the experimental stress of acute pancreatitis leads to increased acinar cell death
308 with ensuing immune cell infiltration and edema.
309

310 **Discussion**

311 When subjected to stress, such as occurring during chronic pancreatitis, acinar cells
312 dedifferentiate and acquire a ductal cell-like phenotype, rendering them prone to *Kras*
313 induced transformation, in contrast to the native duct cells which seem more resistant
314 to neoplastic development. Where studies in the past focused on the acinar cell
315 plasticity and on how the dedifferentiated acinar cells become duct-like (13), the
316 inherent differences between the two cell populations that may underly a different
317 propensity to tumor formation remained unclear. Therefore, we profiled, for the first
318 time to our knowledge, the transcriptome of human dedifferentiated acinar cells versus
319 their native duct cell counterpart. This comparative transcriptomic analysis provided

320 several new insights, including the fact that both cell populations were enriched in
321 'Pathways of cancer' although the related genes differed in both fractions. We identified
322 MECOM, a transcription factor known to be involved in (pancreatic) cancer, as the
323 most uniquely expressed gene in the dedifferentiated acinar cells.
324 MECOM is known to regulate many aspects of tumorigenesis including differentiation,
325 proliferation and apoptosis (17-19, 40). It is a regulator of stomach-specific genes,
326 some of which become upregulated in dedifferentiated acinar cells (23). Previously, a
327 role for MECOM in pancreas cancer was proposed (20, 21, 37). Here, we focused on
328 its role in acinar cell dedifferentiation. We uncovered that MECOM is uniquely
329 expressed in dedifferentiated mouse and human acinar cells and absent from native
330 duct cells, both in cell cultures and in tissue samples. Notably, MECOM expression
331 levels appeared even higher in embryonic mouse pancreas, specifically in the pro-
332 acinar tip cells again suggesting a relation to an immature acinar cell phenotype.
333 Interestingly, SOX9 is a known regulator of acinar cell dedifferentiation and a driver of
334 pancreatic tumor formation (21, 48). Here, SOX9 expression correlated with that of
335 MECOM. An interplay of MECOM and SOX9 has been described in other tissues (12,
336 13, 44) and we confirmed that SOX9 transactivates the *Mecom* enhancer in an acinar
337 cell context. Still, it requires further investigation why SOX9 does not transactivate
338 MECOM expression in duct cells where SOX9 expression is the highest.
339 We observed a clear phenotype when culturing MECOM deficient acinar cells (266-6
340 cells and primary mouse and human acinar cells), i.e. impaired formation of acinar
341 domes or cell clusters, suggesting impaired cell adhesion and higher rates of
342 apoptosis. We showed that MECOM depletion reduced the cell-cell interactions
343 through *Itga2* and its ligands such as *Col4a2*. In our MECOM KO cells, the expression
344 of several integrins (*Itga2, Itga4, Itga5 and Itga9*) was decreased. Importantly,

345 available ChIP-Seq data of MECOM in human ovarian carcinoma cells also showed
346 direct binding to the promotor regions of *Col4a2* and *Itga2* (43). We confirmed this in
347 MECOM KO cells, where reduced activity of the ERK signaling pathway could be
348 directly linked to reduced acinar cell dedifferentiation, a process for which this signaling
349 pathway is critical (12, 44). In a caerulein-induced acute pancreatitis model in MECOM-
350 deficient mice, we again make similar observations and demonstrated a prolonged
351 immune cell infiltration, similar as reported recently (37).
352 We propose that normal acinar cells have two options when they are subjected to
353 stress, either to subside in an "incognito" reversible dedifferentiated state, or to die.
354 MECOM seems indispensable for the former option. Ye et al., who, like us did not
355 provide formal proof by lineage tracing, claimed that MECOM-deficient acinar cells
356 transdifferentiate more extensively during pancreatitis (37). We suggest that MECOM-
357 deficient acinar cells undergo apoptosis and therefore cannot contribute any longer to
358 the CK19+ transdifferentiated cell pool. This is supported by our observations
359 increased inter-acinar spaces filled with fluid (edema) in the acute pancreatitis model.
360 Such phenotype has also been reported in EGF knockout mice (49). We also did not
361 detect any increase in collagen deposition around the recovering acini, which clearly
362 differs from acinar to ductal transdifferentiation that is accompanied by typical collagen
363 deposition (50), further supporting our conclusion.
364 Altogether, these results show that dedifferentiated acinar cells have a clearly distinct
365 gene expression profile compared to native duct cells. Under stress, MECOM
366 expression is turned on, downstream of SOX9, where it prevents acinar cell death and
367 allowing cellular dedifferentiation.
368
369

370 **Acknowledgements**

371 Biospecimens and clinical data were provided by the Australian Pancreatic Cancer
372 Genome Initiative (APGI, www.pancreaticcancer.net.au), which is supported by an
373 Avner Pancreatic Cancer Foundation Grant (www.avnersfoundation.org.au).
374 This work was supported by the Research Foundation Flanders (FWO) (Odysseus
375 project and FWO research project to IR (FWOODYS12 and FWOAL931)). We thank
376 Gunter Leuckx, Emmy De Blay, Veerle Laurysens, Geert Stangé, the laboratory of
377 Liver Cell Biology Research Group at Vrije Universiteit Brussel and Flemish Institute
378 of Biotechnology for expert technical assistance. We thank Patrick Jacquemin for
379 providing the ElaCreERT mice, and Susumu Goyama and Mineo Kurokawa for
380 providing the Evi-1 floxed mice.

381

382 **Conflict of interest**

383 The authors declare no competing financial interests

384
385

386 **References**

387 1. Rahib L, Smith BD, Aizenberg R, Rosenzweig AB, Fleshman JM, Matrisian LM.
388 Projecting cancer incidence and deaths to 2030: the unexpected burden of thyroid,
389 liver, and pancreas cancers in the United States. Cancer Res. 2014;74(11):2913-21.

390 2. Krah NM, De La OJ, Swift GH, Hoang CQ, Willet SG, Chen Pan F, et al. The
391 acinar differentiation determinant PTF1A inhibits initiation of pancreatic ductal
392 adenocarcinoma. Elife. 2015;4.

393 3. Direnzo D, Hess DA, Damsz B, Hallett JE, Marshall B, Goswami C, et al.
394 Induced Mist1 expression promotes remodeling of mouse pancreatic acinar cells.
395 Gastroenterology. 2012;143(2):469-80.

396 4. von Figura G, Morris JPt, Wright CV, Hebrok M. Nr5a2 maintains acinar cell
397 differentiation and constrains oncogenic Kras-mediated pancreatic neoplastic
398 initiation. Gut. 2014;63(4):656-64.
399 5. Kopp JL, von Figura G, Mayes E, Liu FF, Dubois CL, Morris JPt, et al.
400 Identification of Sox9-dependent acinar-to-ductal reprogramming as the principal
401 mechanism for initiation of pancreatic ductal adenocarcinoma. Cancer Cell.
402 2012;22(6):737-50.
403 6. De La OJ, Emerson LL, Goodman JL, Froebe SC, Illum BE, Curtis AB, et al.
404 Notch and Kras reprogram pancreatic acinar cells to ductal intraepithelial neoplasia.
405 Proc Natl Acad Sci U S A. 2008;105(48):18907-12.
406 7. Habbe N, Shi G, Meguid RA, Fendrich V, Esni F, Chen H, et al. Spontaneous
407 induction of murine pancreatic intraepithelial neoplasia (mPanIN) by acinar cell
408 targeting of oncogenic Kras in adult mice. Proc Natl Acad Sci U S A.
409 2008;105(48):18913-8.
410 8. Tuveson DA, Zhu L, Gopinathan A, Willis NA, Kachatrian L, Grochow R, et al.
411 Mist1-KrasG12D knock-in mice develop mixed differentiation metastatic exocrine
412 pancreatic carcinoma and hepatocellular carcinoma. Cancer Res. 2006;66(1):242-7.
413 9. Grippo PJ, Nowlin PS, Demeure MJ, Longnecker DS, Sandgren EP.
414 Preinvasive pancreatic neoplasia of ductal phenotype induced by acinar cell targeting
415 of mutant Kras in transgenic mice. Cancer Res. 2003;63(9):2016-9.
416 10. Guerra C, Schuhmacher AJ, Canamero M, Grippo PJ, Verdaguer L, Perez-
417 Gallego L, et al. Chronic pancreatitis is essential for induction of pancreatic ductal
418 adenocarcinoma by K-Ras oncogenes in adult mice. Cancer Cell. 2007;11(3):291-302.

419 11. Baldan J, Houbracken I, Rooman I, Bouwens L. Adult human pancreatic acinar
420 cells dedifferentiate into an embryonic progenitor-like state in 3D suspension culture.
421 Sci Rep. 2019;9(1):4040.
422 12. Houbracken I, de Waele E, Lardon J, Ling Z, Heimberg H, Rooman I, et al.
423 Lineage tracing evidence for transdifferentiation of acinar to duct cells and plasticity of
424 human pancreas. Gastroenterology. 2011;141(2):731-41, 41 e1-4.
425 13. Pinho AV, Rooman I, Reichert M, De Medts N, Bouwens L, Rustgi AK, et al.
426 Adult pancreatic acinar cells dedifferentiate to an embryonic progenitor phenotype with
427 concomitant activation of a senescence programme that is present in chronic
428 pancreatitis. Gut. 2011;60(7):958-66.
429 14. Roy N, Malik S, Villanueva KE, Urano A, Lu X, Von Figura G, et al. Brg1
430 promotes both tumor-suppressive and oncogenic activities at distinct stages of
431 pancreatic cancer formation. Genes Dev. 2015;29(6):658-71.
432 15. Lee AYL, Dubois CL, Sarai K, Zarei S, Schaeffer DF, Sander M, et al. Cell of
433 origin affects tumor development and phenotype in pancreatic ductal adenocarcinoma.
434 Gut. 2018.
435 16. Pinho AV, Chantrill L, Rooman I. Chronic pancreatitis: a path to pancreatic
436 cancer. Cancer Lett. 2014;345(2):203-9.
437 17. Konantz M, Andre MC, Ebinger M, Grauer M, Wang H, Grzywna S, et al. EVI-1
438 modulates leukemogenic potential and apoptosis sensitivity in human acute
439 lymphoblastic leukemia. Leukemia. 2013;27(1):56-65.
440 18. Rommer A, Steinmetz B, Herbst F, Hackl H, Heffeter P, Heilos D, et al. EVI1
441 inhibits apoptosis induced by antileukemic drugs via upregulation of
442 CDKN1A/p21/WAF in human myeloid cells. PLoS One. 2013;8(2):e56308.

443 19. Glass C, Wuertzer C, Cui X, Bi Y, Davuluri R, Xiao YY, et al. Global Identification
444 of EVI1 Target Genes in Acute Myeloid Leukemia. PLoS One. 2013;8(6):e67134.
445 20. Tanaka M, Ishikawa S, Ushiku T, Morikawa T, Isagawa T, Yamagishi M, et al.
446 EVI1 modulates oncogenic role of GPC1 in pancreatic carcinogenesis. Oncotarget.
447 2017;8(59):99552-66.
448 21. Tanaka M, Suzuki HI, Shibahara J, Kunita A, Isagawa T, Yoshimi A, et al. EVI1
449 oncogene promotes KRAS pathway through suppression of microRNA-96 in
450 pancreatic carcinogenesis. Oncogene. 2014;33(19):2454-63.
451 22. Desai BM, Oliver-Krasinski J, De Leon DD, Farzad C, Hong N, Leach SD, et al.
452 Preexisting pancreatic acinar cells contribute to acinar cell, but not islet beta cell,
453 regeneration. J Clin Invest. 2007;117(4):971-7.
454 23. Grimont A, Pinho AV, Cowley MJ, Augereau C, Mawson A, Giry-Laterriere M,
455 et al. SOX9 regulates ERBB signalling in pancreatic cancer development. Gut.
456 2015;64(11):1790-9.
457 24. Goyama S, Yamamoto G, Shimabe M, Sato T, Ichikawa M, Ogawa S, et al. Evi-
458 1 is a critical regulator for hematopoietic stem cells and transformed leukemic cells.
459 Cell Stem Cell. 2008;3(2):207-20.
460 25. MacDonald RJ, Swift GH, Real FX. Transcriptional control of acinar
461 development and homeostasis. Prog Mol Biol Transl Sci. 2010;97:1-40.
462 26. Baer R, Cintas C, Dufresne M, Cassant-Sourdy S, Schonhuber N, Planque L,
463 et al. Pancreatic cell plasticity and cancer initiation induced by oncogenic Kras is
464 completely dependent on wild-type PI 3-kinase p110alpha. Genes Dev.
465 2014;28(23):2621-35.

466 27. Elghazi L, Weiss AJ, Barker DJ, Callaghan J, Staloch L, Sandgren EP, et al.
467 Regulation of pancreas plasticity and malignant transformation by Akt signaling.
468 Gastroenterology. 2009;136(3):1091-103.
469 28. Wu CY, Carpenter ES, Takeuchi KK, Halbrook CJ, Peverley LV, Bien H, et al.
470 PI3K regulation of RAC1 is required for KRAS-induced pancreatic tumorigenesis in
471 mice. Gastroenterology. 2014;147(6):1405-16 e7.
472 29. Shi ZD, Lee K, Yang D, Amin S, Verma N, Li QV, et al. Genome Editing in
473 hPSCs Reveals GATA6 Haploinsufficiency and a Genetic Interaction with GATA4 in
474 Human Pancreatic Development. Cell Stem Cell. 2017;20(5):675-88 e6.
475 30. Tiyaboonchai A, Cardenas-Diaz FL, Ying L, Maguire JA, Sim X, Jobaliya C, et
476 al. GATA6 Plays an Important Role in the Induction of Human Definitive Endoderm,
477 Development of the Pancreas, and Functionality of Pancreatic beta Cells. Stem Cell
478 Reports. 2017;8(3):589-604.
479 31. Martinelli P, Carrillo-de Santa Pau E, Cox T, Sainz B, Jr., Dusetti N, Greenhalf
480 W, et al. GATA6 regulates EMT and tumor dissemination, and is a marker of response
481 to adjuvant chemotherapy in pancreatic cancer. Gut. 2017;66(9):1665-76.
482 32. Martinelli P, Madriles F, Canamero M, Pau EC, Pozo ND, Guerra C, et al. The
483 acinar regulator Gata6 suppresses KrasG12V-driven pancreatic tumorigenesis in
484 mice. Gut. 2016;65(3):476-86.
485 33. Longoni N, Kunderfranco P, Pellini S, Albino D, Mello-Grand M, Pinton S, et al.
486 Aberrant expression of the neuronal-specific protein DCDC2 promotes malignant
487 phenotypes and is associated with prostate cancer progression. Oncogene.
488 2013;32(18):2315-24, 24 e1-4.

489 34. Izutsu K, Kurokawa M, Imai Y, Maki K, Mitani K, Hirai H. The corepressor CtBP
490 interacts with Evi-1 to repress transforming growth factor beta signaling. Blood.
491 2001;97(9):2815-22.
492 35. Yuasa H, Oike Y, Iwama A, Nishikata I, Sugiyama D, Perkins A, et al. Oncogenic
493 transcription factor Evi1 regulates hematopoietic stem cell proliferation through GATA-
494 2 expression. EMBO J. 2005;24(11):1976-87.
495 36. Buonamici S, Chakraborty S, Senyuk V, Nucifora G. The role of EVI1 in normal
496 and leukemic cells. Blood Cells Mol Dis. 2003;31(2):206-12.
497 37. Ye J, Huang A, Wang H, Zhang AMY, Huang X, Lan Q, et al. PRDM3 attenuates
498 pancreatitis and pancreatic tumorigenesis by regulating inflammatory response. Cell
499 Death & Disease. 2020;11(3):187.
500 38. Schaffer AE, Freude KK, Nelson SB, Sander M. Nkx6 transcription factors and
501 Ptf1a function as antagonistic lineage determinants in multipotent pancreatic
502 progenitors. Dev Cell. 2010;18(6):1022-9.
503 39. Zhou Q, Law AC, Rajagopal J, Anderson WJ, Gray PA, Melton DA. A
504 multipotent progenitor domain guides pancreatic organogenesis. Dev Cell.
505 2007;13(1):103-14.
506 40. Garside VC, Cullum R, Alder O, Lu DY, Vander Werff R, Bilenky M, et al. SOX9
507 modulates the expression of key transcription factors required for heart valve
508 development. Development. 2015;142(24):4340-50.
509 41. Mateo F, Arenas EJ, Aguilar H, Serra-Musach J, de Garibay GR, Boni J, et al.
510 Stem cell-like transcriptional reprogramming mediates metastatic resistance to mTOR
511 inhibition. Oncogene. 2017;36(19):2737-49.

512 42. Jensen JN, Cameron E, Garay MV, Starkey TW, Gianani R, Jensen J.
513 Recapitulation of elements of embryonic development in adult mouse pancreatic
514 regeneration. Gastroenterology. 2005;128(3):728-41.
515 43. Bard-Chapeau EA, Jeyakani J, Kok CH, Muller J, Chua BQ, Gunaratne J, et al.
516 Ecotopic viral integration site 1 (EVI1) regulates multiple cellular processes important
517 for cancer and is a synergistic partner for FOS protein in invasive tumors. Proc Natl
518 Acad Sci U S A. 2012;109(6):2168-73.
519 44. Collins MA, Yan W, Sebolt-Leopold JS, Pasca di Magliano M. MAPK signaling
520 is required for dedifferentiation of acinar cells and development of pancreatic
521 intraepithelial neoplasia in mice. Gastroenterology. 2014;146(3):822-34 e7.
522 45. Means AL, Meszoely IM, Suzuki K, Miyamoto Y, Rustgi AK, Coffey RJ, Jr., et
523 al. Pancreatic epithelial plasticity mediated by acinar cell transdifferentiation and
524 generation of nestin-positive intermediates. Development. 2005;132(16):3767-76.
525 46. Stanger BZ, Stiles B, Lauwers GY, Bardeesy N, Mendoza M, Wang Y, et al.
526 Pten constrains centroacinar cell expansion and malignant transformation in the
527 pancreas. Cancer Cell. 2005;8(3):185-95.
528 47. Strobel O, Dor Y, Alsina J, Stirman A, Lauwers G, Trainor A, et al. In vivo lineage
529 tracing defines the role of acinar-to-ductal transdifferentiation in inflammatory ductal
530 metaplasia. Gastroenterology. 2007;133(6):1999-2009.
531 48. Tanaka M, Shibahara J, Ishikawa S, Ushiku T, Morikawa T, Shinozaki-Ushiku
532 A, et al. EVI1 expression is associated with aggressive behavior in intrahepatic
533 cholangiocarcinoma. Virchows Arch. 2019;474(1):39-46.
534 49. Ardito CM, Grüner BM, Takeuchi KK, Lubeseder-Martellato C, Teichmann N,
535 Mazur PK, et al. EGF receptor is required for KRAS-induced pancreatic tumorigenesis.
536 Cancer Cell. 2012;22(3):304-17.

537 50. Hamada S, Masamune A. Elucidating the link between collagen and pancreatic
538 cancer: what's next? Expert Rev Gastroenterol Hepatol. 2018;12(4):315-7.
539

540 **Figure Legends**
541

542 **Figure 1. RNAseq analysis identifies *MECOM* as uniquely expressed in**
543 **dedifferentiated acinar cells.** (a) Schematic overview of FACS-purification of human
544 dedifferentiated acinar and duct cells, using acinar-specific UEA-1 lectin. (b)
545 Immunofluorescent staining of FACS-purified dedifferentiated acinar (UEA-1+/CA19.9-
546) and duct (UEA-1-/CA19.9+) cells at day 4 with CD142 and CA19.9. DNA is labelled
547 in blue. (c) Table of genes uniquely expressed in human dedifferentiated acinar cells
548 (green) and duct cells. Selection limited to genes with BaseMean ≥ 1000, Log2FC ≥ 2
549 or ≤ -2 and P.adj ≤ 0,01. (d) KEGG pathways enriched (Adj. p-value < 0,01) in human
550 dedifferentiated acinar cells (N=5).
551

552 **Figure 2. MECOM is uniquely upregulated in dedifferentiated acinar cells and not**
553 **in duct cells.** (a) qPCR for MECOM on purified human dedifferentiated acinar (UEA-
554 1+/CA19.9-) versus duct cells (UEA-1-/CA19.9+) after FACS isolation at day 4 of
555 culture, compared to the mixed exocrine fraction at day of isolation (D0) (N=5; mean ±
556 SD; ***p<0,005; One-way ANOVA with post-hoc Bonferroni correction). (b,c) RNA-ISH
557 for MECOM on tissue from normal human pancreas (b) and human chronic pancreatitis
558 (c) Scale = 50μM. Arrows indicate individual mRNA dots. (d,e) Immunofluorescent co-
559 staining of human mixed exocrine fraction at day 4 of culture for MECOM and CD142
560 (d) and for MECOM and CK19 (e). Scale = 50μM. (f-i) RNA-ISH for *Mecom* and (j)
561 *Mecom* expression level in normal mouse pancreas (f; dotted line indicates a normal
562 duct, striped line indicates the outer edge of an islet), embryonic pancreas (g); E16.5

563 embryonic pancreas; dashed line indicates groups of tip cells) and in a mouse model
564 for acute (h) and chronic (i) pancreatitis. Scale = 50μM. (j) 5 individual microscopic
565 fields per replicate were quantified. (N=5; mean ± SD; *p<0,05; **p<0,01; One-way
566 ANOVA with post-hoc Bonferroni correction;).
567
568 **Figure 3. SOX9 regulates MECOM during acinar cell dedifferentiation.** (a) qPCR
569 for MECOM and SOX9 expression on human exocrine mixed fraction in culture over
570 time (day 1 to day 8). Each donor is indicated as a different colored line. (b) Immunoblot
571 for MECOM, SOX9 and actin as loading control on human exocrine mixed fraction in
572 culture over time. Representative blot from N=3 human donor samples. The different
573 isoforms of MECOM locus are indicated by arrows. (c) Generation of acinar-specific
574 (Elastase) Cre deletor mice with $Sox9^{ex5}$ flanked by loxP sites. Acinar-specific deletion
575 of SOX9 is performed in ElaCreERT;$Sox9^{f/f}$ versus control (ElaCreERT) littermates by
576 administering tamoxifen 3 times over a period of 5 days, followed by a two-week
577 washout. Acute pancreatitis is induced by administering caerulein by 7 hourly injections
578 for 3 days over a period of 5 days. Mice are sacrificed at day 4 after caerulein
579 administration. Immunohistochemical staining for SOX9 and RNA in situ hybridization
580 of *Mecom* mRNA expression in mouse pancreatic tissue after experimentally induced
581 acute pancreatitis in control (ElaCreERT) and acinar-specific Sox9 knockout
582 (ElaCreERT;$Sox9^{f/f}$) mice. Scale = 50μM. (N=3; **p<0.01; unpaired two-tailed t-test)
583 (d) Luciferase reporter assay in 266-6 cells, 48h after transfection. (mean ± SD; N=3;
584 ***p<0,001; one-way ANOVA with post-hoc Bonferroni correction)
585
586 **Figure 4. *Mecom* retains cell adhesion and survival in 266-6 cells.** (a) RNA in situ
587 hybridization (RISH) on control (NT-gRNA) and Mecom KO (gRNA3) 266-6 cells. Scale

588 = 200μM. (N=3; **p<0,01; unpaired two-tailed t-test). (b) Phase contrast images of
589 control (NT-gRNA) and Mecom KO (gRNA3) 266-6 cells. Scale = 200μM. (c) Absolute
590 number of cells at 96h after seeding 50.000 cells (mean ± SD; N=3; **p<0,01; unpaired
591 two-tailed t-test) (d) Cell viability measured relative to background levels of the culture
592 medium by CellTiter Glo assay (mean ± SD; N=3; ***p<0,001; unpaired two-tailed t-
593 test) (e) Immunofluorescent staining and quantification of cleaved caspase 3+ cells.
594 (N=3; **p<0,01; unpaired two-tailed t-test) (f) KEGG pathway analysis on differential
595 gene expression profiles after RNAseq analysis of MECOM wildtype versus MECOM
596 KO cells (N=3) (g) Venn diagrams showing genes overlapping between differentially
597 expressed genes in MECOM KO 266-6 cells and publicly available ChIP-seq dataset
598 from Bard-Chapeau et al. (43) (h) Schematic representation of our hypothesis. (i)
599 Collagen IV immunofluorescent staining on 266-6 NTgRNA and gRNA3-transduced
600 cultured cells. (j) Immunoblot for phospho-ERK and total ERK and quantifications of
601 pERK relative to total protein stain. (mean ± SD; N=3; *p<0,05; Unpaired two-tailed t-
602 test)
603
604 **Figure 5. *Mecom* retains cell adhesion and survival in cultured acinar cells.** (a)
605 Acinar cell-specific deletion of MECOM is performed by administering tamoxifen 3
606 times over a period of 5 days both subcutaneously and by gavage, followed by a two-
607 week washout period. Acute pancreatitis is induced by administering caerulein by 7
608 hourly injections for 3 days over a period of 5 days. Mice are sacrificed at day 4 after
609 caerulein treatment. (b,e) Phase contrast images and quantification of mean cluster
610 surface of ElaCreERT and ElaCreERT;*Mecom*$^{f/f}$ isolated acinar cells immediately after
611 isolation (D0) and at day 4 of culture (D4). Scale = 100μM. (c,f) Cleaved caspase 3
612 staining and quantification on ElaCreERT and ElaCreERT;*Mecom*$^{f/f}$ acinar cells at day

613 4 of culture. Scale = 25μM. *(*d,g) CK19 staining and quantification of ElaCreERT and
614 ElaCreERT;*Mecom*$^{f/f}$ acinar cells at day 4 of culture. Scale = 25μM. (mean ± SD; N=6;
615 *p<0,05; **p<0,01; two-way ANOVA with post-hoc Bonferroni correction.)
616
617 **Figure 6. *Mecom* depletion in acinar cells *in vivo* causes pronounced cell death**
618 **during recovery after caerulein-induced acute pancreatitis.** (a) Acinar-specific
619 deletion of MECOM is performed by administering tamoxifen 3 times over a period of
620 5 days, followed by a two-week washout period. Acute pancreatitis is induced by
621 administering caerulein by 7 hourly injections for 3 days over a period of 5 days. Mice
622 are sacrificed at day 4 and day 11 after caerulein administration. (b,f) H&E staining
623 and quantification of acinar/non-acinar area ratio relative to day 4. (c,g) Cleaved
624 caspase 3 immunohistochemical staining and quantification at day 4. (d,h) Collagen
625 staining and quantification relative to day 4. Scale = 50μM. (e,i) CD3 staining and
626 quantification relative to day 4 for ElaCreERT and ElaCreERT;*Mecom*$^{f/f}$ mice. Scale =
627 50μM. (mean ± SD, N=6, **p<0,01, ns = non-significant. two-way ANOVA with post-
628 hoc Bonferroni correction)
629

Figure 1

a

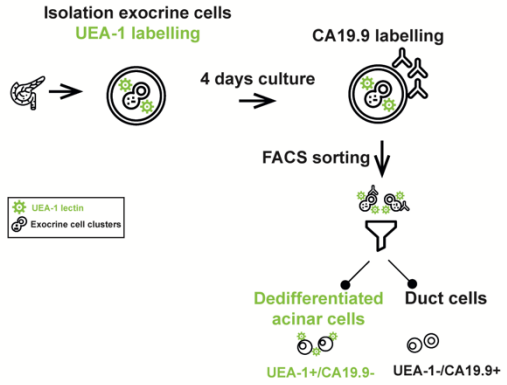

b

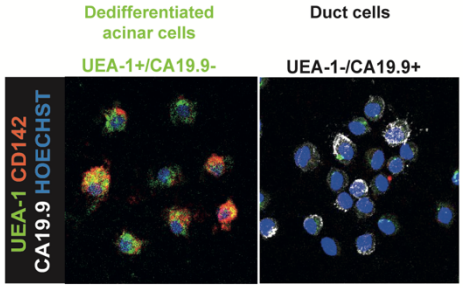

c

Dedifferentiated acinar cells (FC≤-2, adj.P≤0,01)	
Pathway	**Adj.P**
Protein digestion and absorption	1,185208E-11
Pancreatic secretion	1,267413E-10
Metabolic pathways	8,920072E-04
Pathways in cancer	2,494694E-03
Complement and coagulation cascades	2,704916E-03
Metabolism of xenobiotics by cytochrome P450	3,886956E-03
Fat digestion and absorption	3,953574E-03
Mineral absorption	3,953574E-03
PI3K-Akt signaling pathway	4,032070E-03
Drug metabolism - cytochrome P450	5,712517E-03
Steroid hormone biosynthesis	8,027015E-03
Glycine, serine and threonine metabolism	9,867525E-03

d

symbol	log2FoldChange	padj
DCD2	4,178944	7,066393E-126
MXRA5	-5,436366	1,103561E-129
GSTA2	-5,679022	2,094860E-159
IGFBP2	-5,777801	8,550959E-126
MGST1	-5,895840	1,446389E-147
MECOM	-6,091834	1,040978E-123
LGALS2	-4,859710	7,753555E-130

630

Figure 2

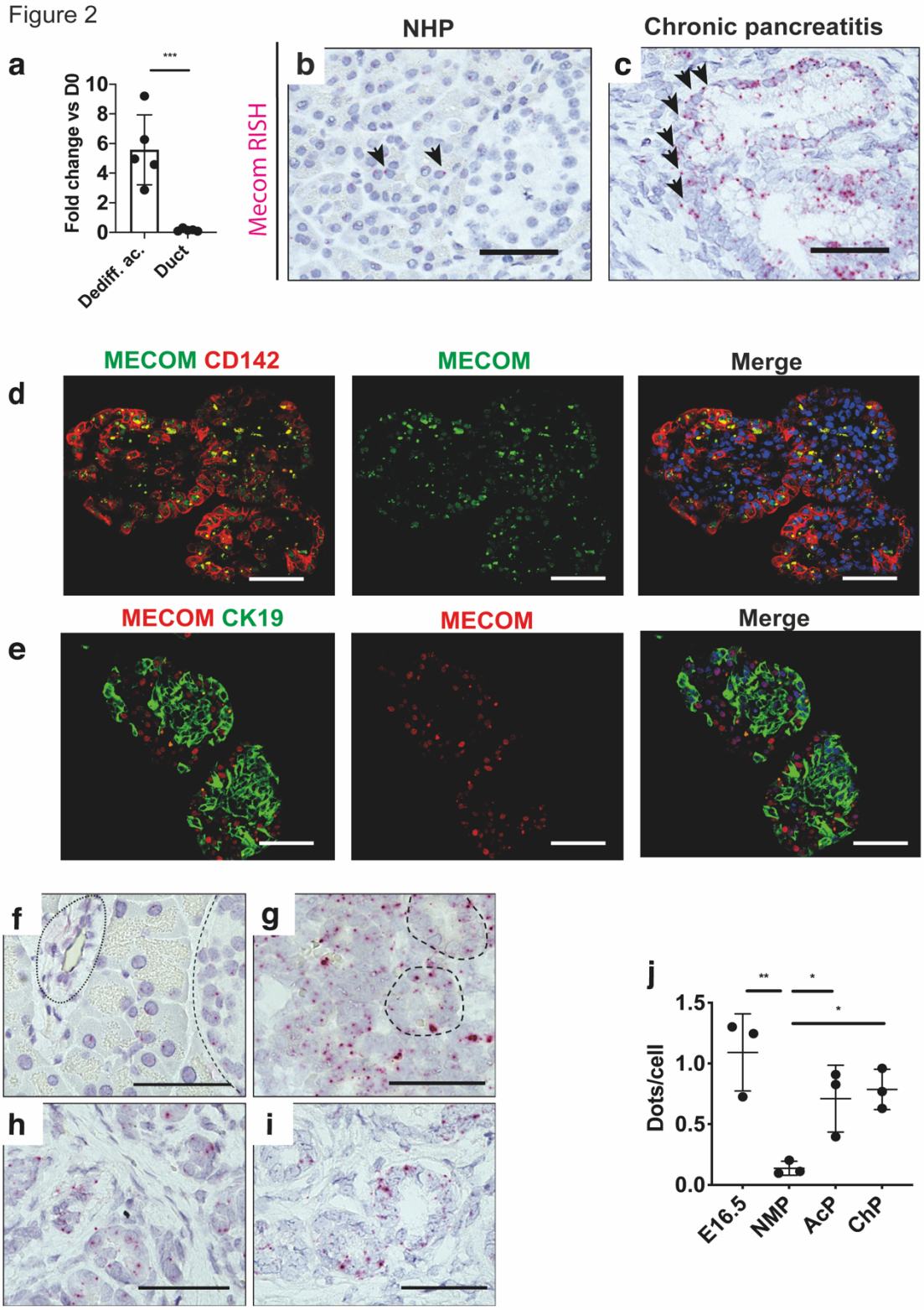
a
Fold change vs D0
10
8
6
4
2
0
***
Dediff. ac.
Duct
Mecom RISH
NHP
Chronic pancreatitis
b
c
d
MECOM CD142
MECOM
Merge
e
MECOM CK19
MECOM
Merge
f
g
h
i
j
Dots/cell
1.5
1.0
0.5
0.0
**
*
*
E16.5
NMP
AcP
ChP

631

Figure 3

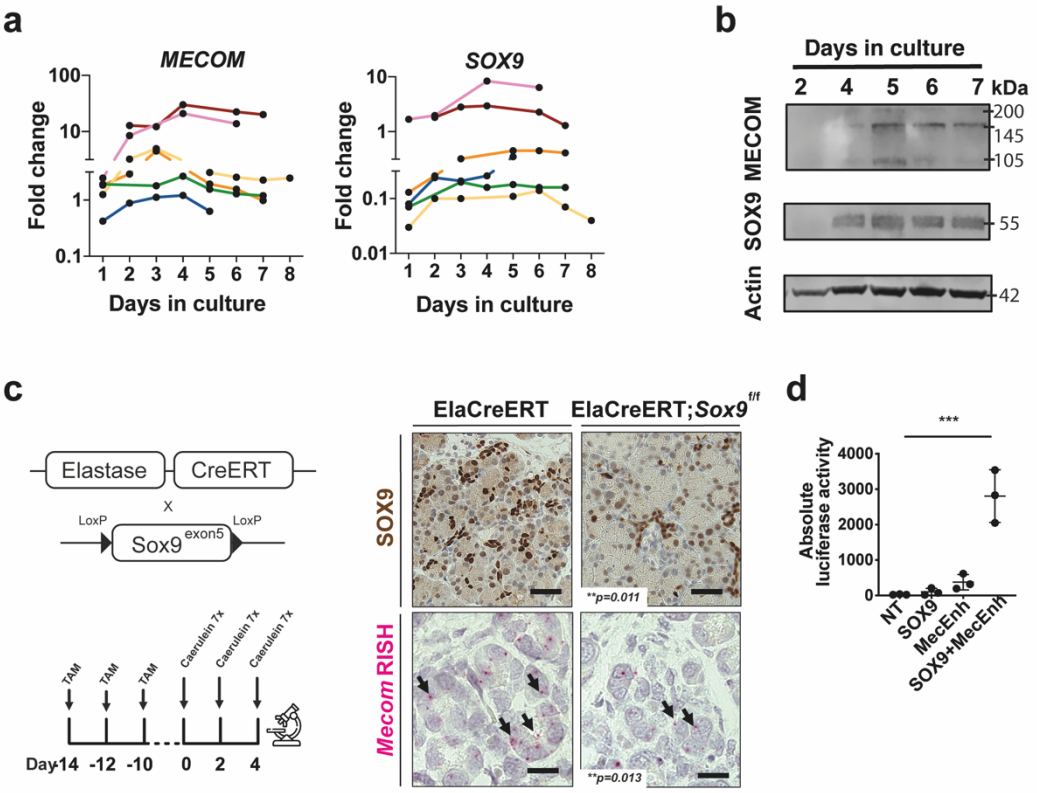
a
MECOM
SOX9
Fold change
Days in culture
b
Days in culture
2 4 5 6 7 kDa
MECOM
SOX9
Actin
200
145
105
55
42
c
Elastase
CreERT
X
LoxP
Sox9 exon5
TAM
Caerulein Tx
Day -14 -12 -10 0 2 4
ElaCreERT
ElaCreERT;Sox9 f/f
SOX9
Mecom RISH
**p=0.011
**p=0.013
d
***
Absolute luciferase activity
NT
SOX9
MecEnh
SOX9+MecEnh

632

Figure 4

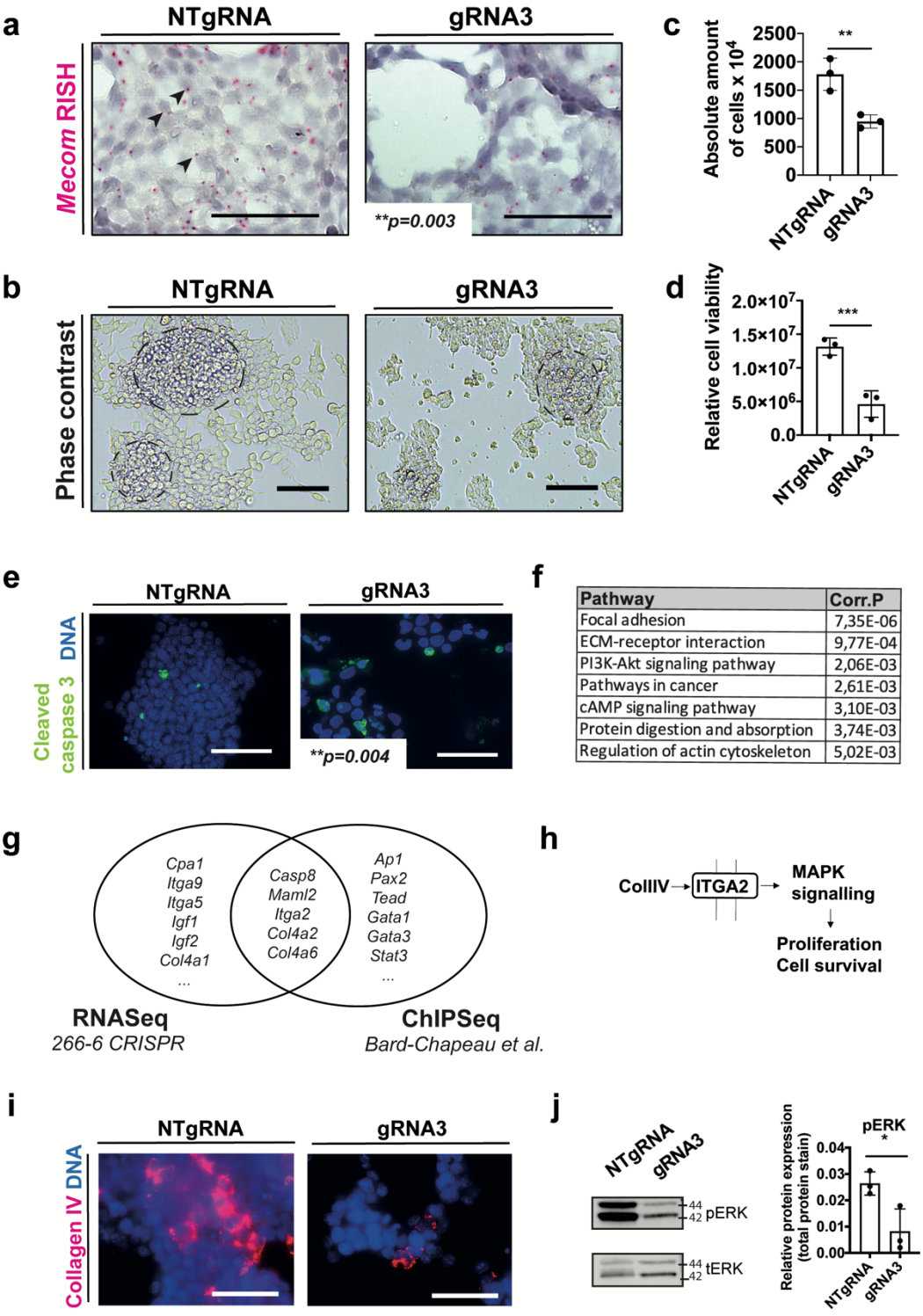

Pathway	Corr.P
Focal adhesion	7,35E-06
ECM-receptor interaction	9,77E-04
PI3K-Akt signaling pathway	2,06E-03
Pathways in cancer	2,61E-03
cAMP signaling pathway	3,10E-03
Protein digestion and absorption	3,74E-03
Regulation of actin cytoskeleton	5,02E-03

633

Figure 5

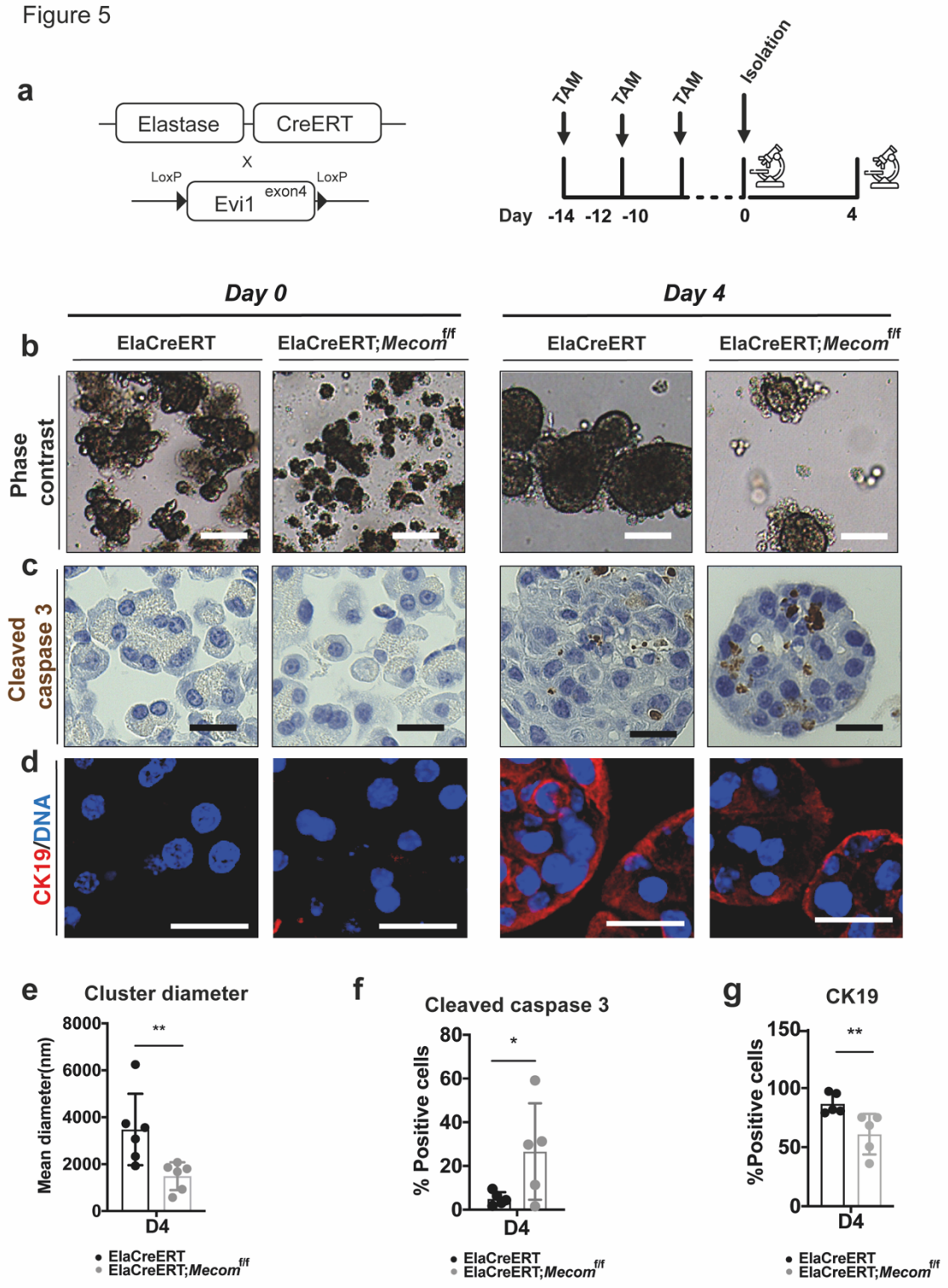
a
Elastase
CreERT
X
LoxP
Evi1
exon4
LoxP
TAM
TAM
TAM
Isolation
Day -14 -12 -10 0 4
Day 0
Day 4
b
ElaCreERT
ElaCreERT;Mecom f/f
ElaCreERT
ElaCreERT;Mecom f/f
Phase contrast
c
Cleaved caspase 3
d
CK19/DNA
e
Cluster diameter
Mean diameter(nm)
8000
6000
4000
2000
0
**
D4
ElaCreERT
ElaCreERT;Mecom f/f
f
Cleaved caspase 3
% Positive cells
80
60
40
20
0
*
D4
ElaCreERT
ElaCreERT;Mecom f/f
g
CK19
%Positive cells
150
100
50
0
**
D4
ElaCreERT
ElaCreERT;Mecom f/f

634

Figure 6

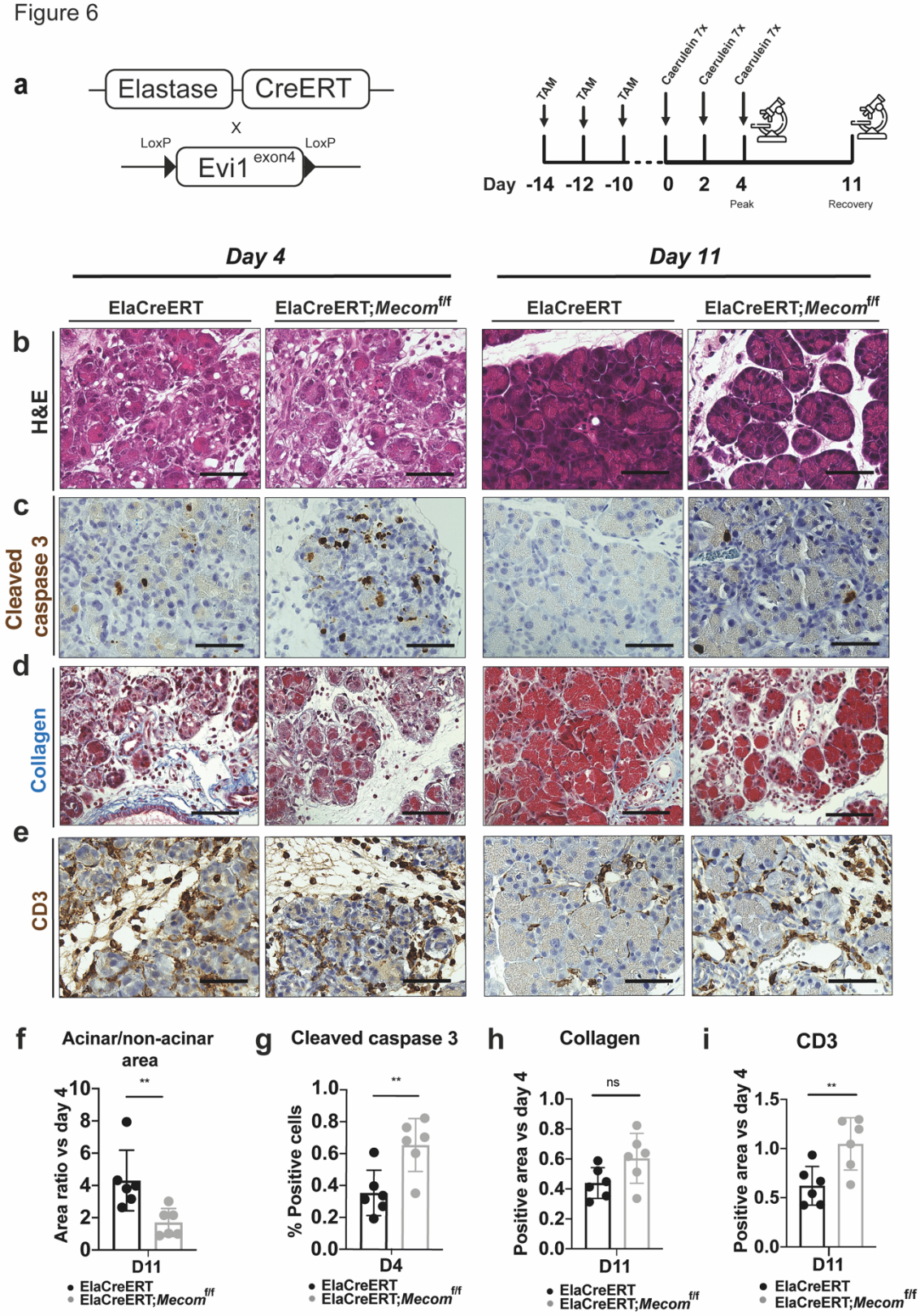
a
Elastase
CreERT
X
LoxP
Evi1 exon4
LoxP
TAM
TAM
TAM
Caerulein Tx
Caerulein Tx
Caerulein Tx
Day -14 -12 -10 0 2 4 11
Peak
Recovery
Day 4
Day 11
ElaCreERT
ElaCreERT;Mecom f/f
ElaCreERT
ElaCreERT;Mecom f/f
b
H&E
c
Cleaved caspase 3
d
Collagen
e
CD3
f
Acinar/non-acinar area
Area ratio vs day 4
D11
ElaCreERT
ElaCreERT;Mecom f/f
g
Cleaved caspase 3
% Positive cells
D4
ElaCreERT
ElaCreERT;Mecom f/f
h
Collagen
Positive area vs day 4
ns
D11
ElaCreERT
ElaCreERT;Mecom f/f
i
CD3
Positive area vs day 4
D11
ElaCreERT
ElaCreERT;Mecom f/f

635